THE UNIVERSITY OF MICHIGAN

COLLEGE OF ENGINEERING
Department of Nuclear Engineering

Technical Report

A THERMAL NEUTRON SPECTRUM MEASURED BY A CRYSTAL SPECTROMETER

J. L. Donovan
J. S. King
P. F. Zweifel

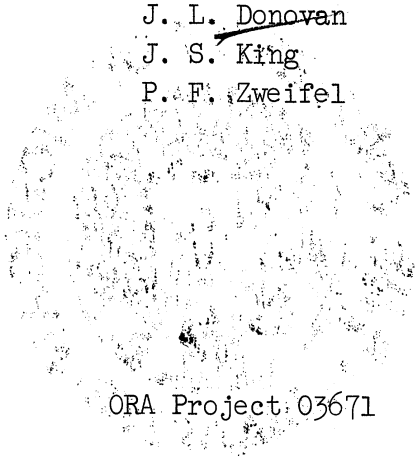

ORA Project 03671

under contract with:

NATIONAL SCIENCE FOUNDATION
GRANT NO. G-12147
WASHINGTON, D. C.

administered through:

OFFICE OF RESEARCH ADMINISTRATION ANN ARBOR

January 1963

ABSTRACT

The thermal neutron spectrum of a beam from a research reactor has been measured using a crystal spectrometer. The relative number of neutrons as a function of Bragg angle was determined. Corrections for background, crystal reflectivity, detector efficiency, and second-order component were applied to the raw data. The first- and second-order flux from the reactor was calculated, and a Maxwellian temperature determined. The first-order monoenergetic flux which is available for inelastic scattering experiments was computed together with an estimate of the second-order contamination as a function of energy.

A. INTRODUCTION

Direct measurement of the leakage spectrum of a neutron beam to obtain the relative number of neutrons as a function of energy can be carried out using either a crystal spectrometer or a mechanical chopper. Because the crystal spectrometer and the mechanical chopper have efficiency corrections and transmission functions that vary as a function of energy, accurate energy distributions are difficult to obtain. For example, analysis of the data obtained using a crystal spectrometer depends on exact knowledge of the crystal reflectivity as a function of energy.

Because of these difficulties, indirect methods are often used to obtain the temperature of the neutron distribution. Often these methods depend on assuming that the energy distribution is a Maxwell-Boltzmann distribution. An example of an indirect method is the use of a boron absorber with high transmission followed by a thin 1/v detector. Because the velocity distribution seen by the detector is assumed Maxwellian, the observed transmission cross section for the entire beam will be the average cross section for the Maxwellian distribution. The observed cross section, together with the known boron cross section, can be used to determine the most probable velocity of the distribution and thus the temperature.

Although the boron absorption method of determining the temperature of the neutron distribution is simple to carry out, the temperature values obtained vary over a range of about 100°C. This may be the result of the assumption of a Maxwellian distribution. Typical results obtained by experimenters at Argonne using this method are temperature values of 330°K and 287°K for the distribution at the thermal column of the Argonne deuterium pile.[1,2] This method was also used to measure the temperature of neutron distributions from deep and shallow holes in the thermal column of the Argonne graphite pile.[3] Values of 293°K and 255°K were obtained.

Measurements of reactor temperatures based on other methods have been reported. Using cadmium and boron absorbers, Anderson reported a temperature at the center of the Argonne graphite pile of 383°K.[4] At Oak Ridge the boron sandwich method was used to measure the temperature inside the Oak Ridge graphite pile.[5] The result was a temperature of 413°K.

Early reports of measurements by groups at Argonne and Oak Ridge, using crystal spectrometers, gave results of 90°C, 100°C and 155°C above moderator temperature.[6,7,8] More recent reports of measurements made with mechanical choppers in England and Sweden gave results of 8°C and 43°C above moderator temperature.[9,10]

B. DESCRIPTION OF THE EQUIPMENT

The Ford Nuclear Reactor is a swimming pool reactor with MTR-type fuel elements. It currently operates at a power level of 1 megawatt, providing neutrons for nuclear research at The University of Michigan. Ten beam tubes are located around the core. The beam tubes begin outside the 3-inch graphite reflector surrounding the core, and penetrate through the concrete shielding wall. The orientation of the beam tubes is shown in Fig. 1.

A triple-axis crystal spectrometer is used with the neutron beam from beam port A. In measuring the leakage spectrum of the neutron beam, this spectrometer is used to determine the spectrum of thermal neutrons incident on the copper crystal inside the spectrometer. The crystal is used to provide a monoenergetic beam of neutrons for inelastic scattering experiments. The neutron beam, after Bragg reflection off the copper crystal, passes through a fission monitor. The beam transmission through this monitor is approximately 98%. The attenuation of the beam is due mainly to the aluminum walls of the monitor; the detection efficiency of the U-235 layer is 10^{-3} at 0.087 ev.

The reflected beam is rectangular in shape at the fission monitor, 2.84 inches high by 2.08 inches wide. For the present experiments a cadmium iris was centered over the face of the monitor to allow the thermal neutrons inside a 1.5-inch-diameter circle to pass into the monitor. To measure the fast-neutron background at each angular position, a full sheet of cadmium was positioned over the face of the monitor.

C. METHOD OF COMPUTATION

Measurements of the total neutron flux and the epicadmium neutron flux at the monitor were made over the energy range 0.025 to 0.293 ev. The count rate obtained by subtracting out the epicadmium neutron background is shown in Fig. 2 for the energy range 0.025 to 0.16 ev. The dips in the measured count are due to destructive interference from competing planes in the crystal. The smooth curve shown fitted to the measured points was used for computation of the thermal spectrum.

The calculated reflectivity $R(\Theta)$ for the (200) planes of the copper crystal is shown in Fig. 3 for first- and second-order reflection as a function of energy. The reflectivity of a crystal used in reflection is calculated from the following experssion:[11]

$$R(\Theta) = \int_{-\infty}^{+\infty} \frac{a\, d\, \Delta}{(1 + a) + (1 + 2a)^{1/2} \coth [A(1 + 2a)^{1/2}]}$$

where $a = Q/\mu \left(1/\eta \sqrt{2\pi}\right) \exp [- \Delta^2/2\eta^2]$

$\Delta = \theta - \theta_B$

$A = (\mu t_o)/(\sin \theta_B)$

$Q = (\lambda^3 N^2 F^2)/(\sin 2\theta_B)$

For these calculations, the following values were used for the copper crystal:

$t_o = 3.8$ cm

$\mu(E) = \Sigma_T(E) - \Sigma_{coh}(E) \simeq \Sigma_a(E) = .319\sqrt{\frac{.025}{E\ (ev)}}$

$F^2(200) = 9.24 \times 10^{-24}$ cm^2

$N^2 = 4.50 \times 10^{44}$ cm^{-6}

$\eta = 2$ minutes $= 5.82 \times 10^{-4}$ radians

The efficiency of the monitor is shown in Fig. 4. This curve is calculated from the known cross section and thickness of the U-235 plating in the fission monitor. The detector efficiency factor and the crystal reflectivity are used with the corrected observed count rate to obtain the spectrum.

ANALYSIS OF THE DATA

The observed count rate at a high energy (0.28 ev) was used to begin the order correction to the raw data. Assume two conditions:

1. The spectrum above 0.28 ev varies as 1/E.

2. Only first- and second-order contributions are important at 0.28 ev; the first-order count rate at 0.28 ev can be computed. Define:

   Observed Count Rate at θ = C.R. (0)
   First-Order Count Rate = C.R. (1)
   Second-Order Count Rate = C.R. (2)
   First-Order Reflectivity, Efficiency: $R^1(\theta)$, $\epsilon^1(\theta)$
   Second-Order Reflectivity, Efficiency: $R^2(\theta)$, $\epsilon^2(\theta)$
   First- and Second-Order Flux: $\phi^1(E)$, $\phi^2(E)$
   First-Order Jacobian: $[dE^1/d\theta] = 2E \cot \theta$
   Second-Order Jacobian: $[dE^2/d\theta] = (2)^2 2E \cot \theta = 8E \cot \theta$

Then,

$$\text{C.R. (0)} = \text{C.R. (1)} + \text{C.R. (2)}$$

$$= \phi^1(E)\, R^1(\theta)\, \epsilon^1(\theta) \frac{d\, E^1}{d\, \theta} + \phi^2(E)\, R^2(\theta)\, \epsilon^2(\theta) \frac{d\, E^2}{d\, \theta} \qquad (1)$$

Now at .28 ev,

$$\phi^2(E) = \frac{\phi^1(E)}{4}$$

and at all energies

$$\left[\frac{d\, E^2}{d\, \theta}\right] = 4 \left[\frac{d\, E^1}{d\, \theta}\right].$$

For the 1/E region, therefore,

$$\text{C.R. (0)} = \phi^1(E)\, 2\, E \cot \theta\, [R^1(\theta)\, \epsilon^1(\theta) + R^2(\theta)\, \epsilon^2(\theta)] \qquad (2)$$

For E = 0.28 ev,

$$690 \text{ counts/min} = \phi^1(E)\, (0.560)\, (6.60)\, [1.698\, (7.40) + 0.98\, (3.66)] \times 10^{-7}$$

or,

$$\phi^1(E) = \frac{690}{3.70\, (16.17) 10^{-7}} = 1.15 \times 10^8 \text{ neutrons/min - } 11.4 \text{ cm}^2$$

$$= 1.68 \times 10^5 \text{ neutrons/cm}^2 \text{ - sec}$$

This value of the flux at 0.28 ev was used to compute the flux up to 1.12 ev; the 1/E flux relationship was used for this energy range. The resulting flux values were then used in Eq. (1) to correct the observed count values from 0.28 ev down to 0.07 ev. Below this energy the raw count was corrected using the corrected raw count for the energy range 0.10 to 0.28 ev.

The first- and second-order flux as a function of Bragg angle, $\phi(\theta)$ was then computed, as follows:

$$\phi^1(\theta) = \frac{\text{corrected count rate}}{R(\theta)\, \epsilon(\theta)} = \frac{\text{C.R. (1)}}{R^1(\theta)\, \epsilon^1(\theta)}$$

The flux as a function of energy is computed as follows:

$$\phi^1(E) = \phi^1(\theta) \frac{d\, \theta}{d\, E^1} = \phi^1(\theta) \frac{1}{2E^1 \cot \theta}$$

TEMPERATURE OF THE SPECTRUM

The flux $\phi^1(\theta)$ is shown in Fig. 5. The temperature T corresponding to this spectrum can be found as follows, assuming a Maxwell-Boltzmann distribution:

$$\phi_{MB}(\theta) = \phi_{MB}(E)\, 2E \cot\theta = K^1 E^2 e^{-E/kT} \cot\theta$$

Now,

$$\lambda = 2d \sin\theta = C^1 E^{-1/2} \quad \text{or} \quad E = C \sin^{-2}\theta$$

where

$$C = \left(\frac{.287}{2d}\right)^2 = \left(\frac{.287}{3.615}\right)^2 \text{ for copper (200) planes.}$$

Then

$$\phi_{MB}(\theta) = \frac{K \cos\theta \exp(-C \sin^{-2}\theta/kT)}{\sin^4\theta \sin\theta} = \frac{K \cos\theta \exp(-C \sin^{-2}\theta/kT)}{\sin^5\theta}$$

$$\frac{d\phi_{MB}(\theta)}{d\theta} = K \exp[-C \sin^{-2}\theta/kT] \left[\frac{2C \cos^2\theta}{kT \sin^8\theta} - \frac{\sin\theta}{\sin^5\theta} - \frac{5\cos^2\theta}{\sin^6\theta}\right] = 0$$

or

$$\frac{2C \cot^2\theta}{kT \sin^2\theta} = 1 + 5\cot^2\theta, \quad kT = \frac{2C}{\sin^2\theta(5 + \tan^2\theta)}$$

From Fig. 5 the peak of the curve is seen to occur at $\theta = 17.6°$. Then

$$kT = \frac{2\left(\frac{.287}{3.615}\right)^2}{(.0916)(5 + 0.10)} = 0.0270 \text{ ev}$$

Another method may be used to obtain the value of kT corresponding to the measured spectrum. It may be noted that, again assuming a Maxwell-Boltzmann distribution,

$$\phi(E) = KEe^{-E/kT}, \text{ or } \frac{\phi(E)}{E} = Ke^{-E/kT}, \ln\left[\frac{\phi(E)}{E}\right] = \ln K - E/kt$$

Therefore, a plot of $\ell n\ [\phi(E)/E]$ vs. E will have a slope of $(-1/kT)$. This analysis is shown as Fig. 6. The slope of the straight line fitted to the points between 0.025 and 0.12 ev corresponds to the value kT = .0268 ev, which is equivalent to a spectrum temperature of 311°K, or 38°C. The above analysis of $\phi^1(\theta)$ corresponds to a spectrum temperature of 313°K, or 40°C.

When the FNR is operated at 1 megawatt, the temperature of the pool water is normally about 82°F, or 27.8°C. In moving thru the core, the temperature rise for the cooling water is 8°F, or 4.4°C.

Figure 7 shows the measured spectrum plotted as a function of energy. For comparison purposes, a Maxwell-Boltzmann distribution corresponding to kT = .027 ev is also shown. It will be noted that the 1/E contribution becomes important above 0.13 ev; it is equal to the Maxwell-Boltzmann contribution at E = 0.215 ev.

The percentage of the observed count rate at the monitor at any energy that is due to first-order neutrons is shown in Fig. 8. From this curve, the magnitude of the correction to be applied to an observed monitor count for calculating the first-order component incident on a target used in an inelastic scattering experiment can be obtained.

Inelastic scattering experiments also require knowledge of the relative flux values at the target as a function of energy. The spectrum measured above is that which is incident on the monochromating crystal. This spectrum is modified after reflection off the copper crystal because of the variation of the crystal reflectivity with energy. The resulting relative intensities of first- and second-order neutrons for the energy range of interest in inelastic scattering experiments are shown in Fig. 9. Figure 10 illustrates the second-order contamination of the beam incident on a scattering target as a function of energy. The percentage of the incident experimental beam which is made up of first-order neutrons is shown as a function of energy for the energy range of interest in inelastic scattering experiments.

Acknowledgment

It is a pleasure to acknowledge the assistance of Mr. W. Myers, who determined the value of η for the copper crystal.

REFERENCES

1. Wattenberg, A. and Jankowski, F., Unpublished Report, Argonne National Laboratory (1949).

2. Hughes, D., Wallace, J., and Haltzmann, R., Phys. Rev. 73, 1277 (1948).

3. Fermi, E., Marshall, J., and Marshall, L., Phys. Rev. 72, 193 (1947).

4. Anderson, H., Fermi, E., Wattenberg, A., Weil, G., and Zinn, W., Phys. Rev. 72, 16 (1947).

5. Branch, G., Manhattan District Document 747: T.I.D., (1946).

6. Zinn, W., Phys. Rev. 71, 752 (1947).

7. Sturm, W., Phys. Rev. 71, 757 (1947).

8. Bernstein, S., Unpublished Report, Oak Ridge (1947).

9. Poole, M., J. Nuc. Energy 5, 325 (1957).

10. Larrson, K., Stedman, R., and Palevsky, H., J. Nuc. Energy 6, 222 (1958).

11. Bacon, G., Neutron Diffraction, P. 69, Oxford Clarendon Press (1962).

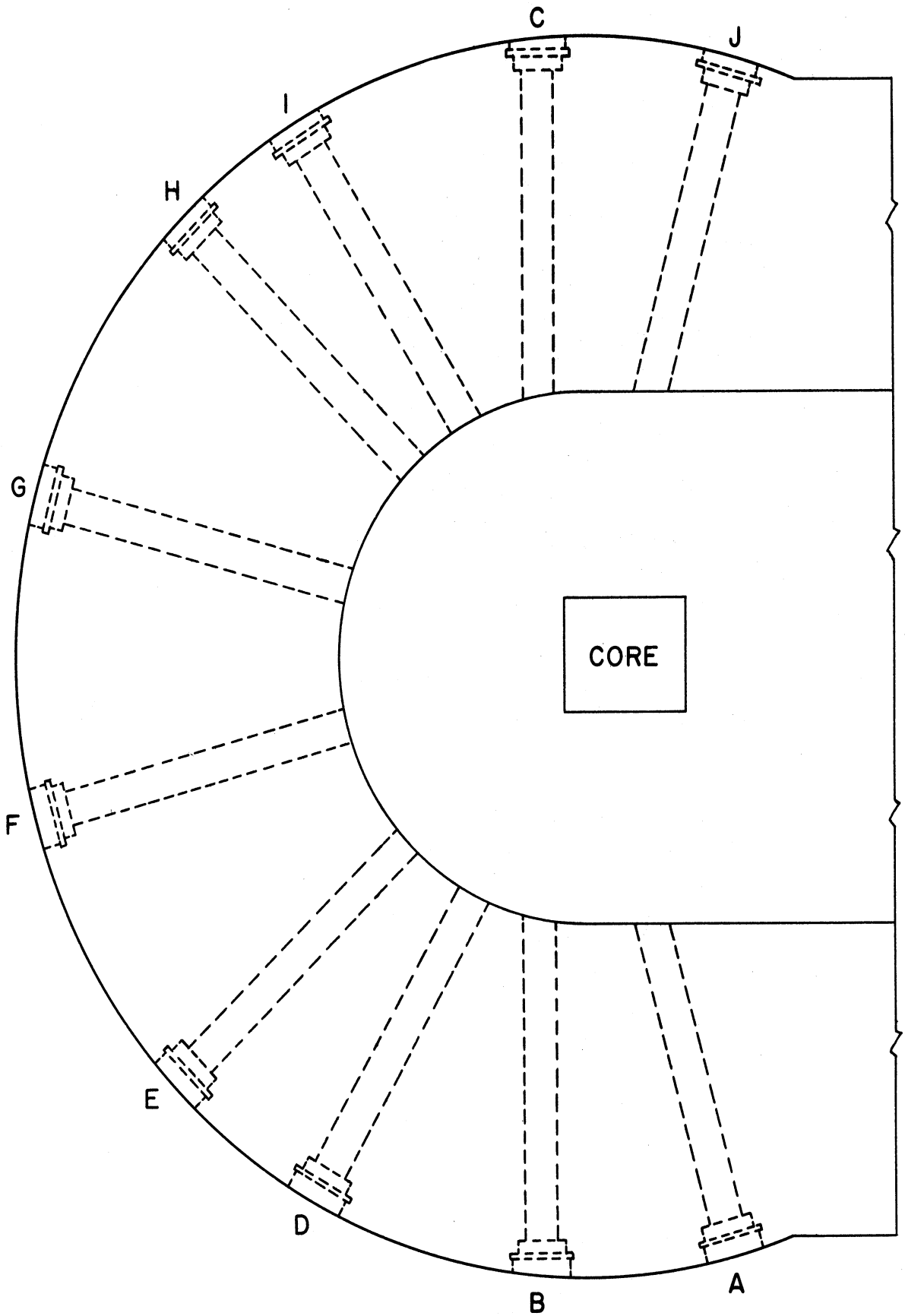

Fig. 1. Beam port arrangement of the Ford Nuclear Reactor.

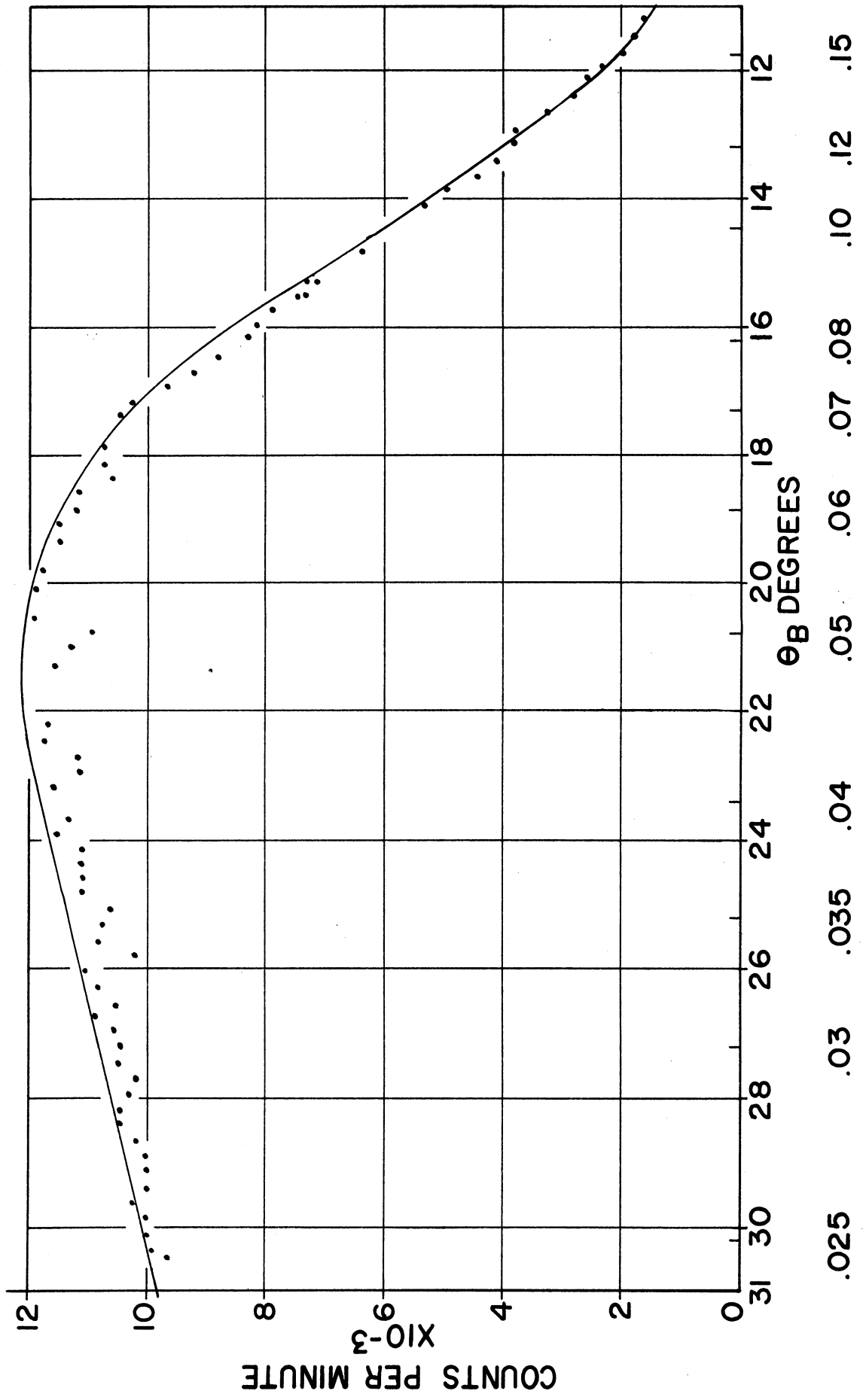

Fig. 2. Count rate of neutron flux for energy range 0.025 to 0.16 ev.

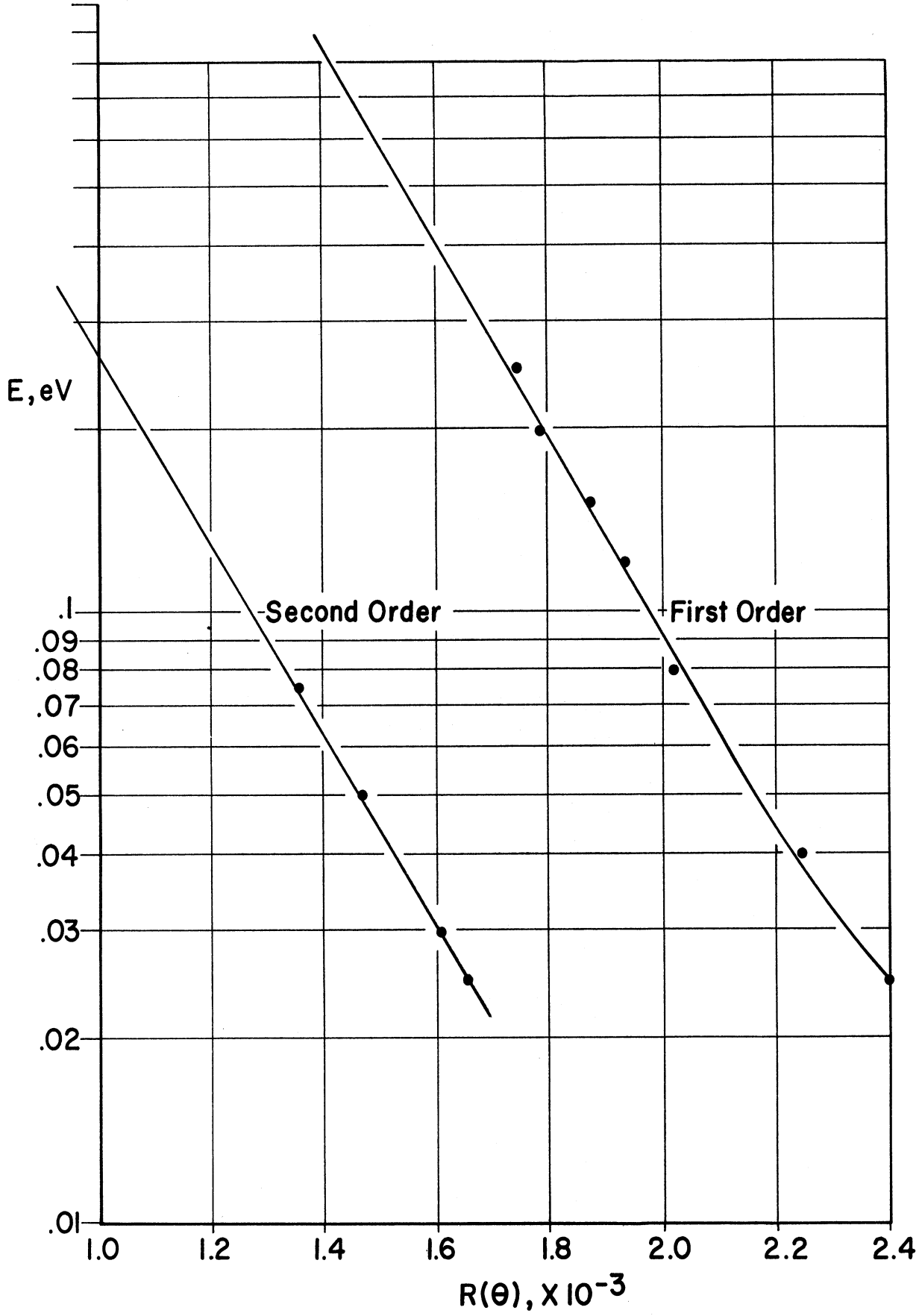

Fig. 3. First- and second-order reflectivity for copper (200).

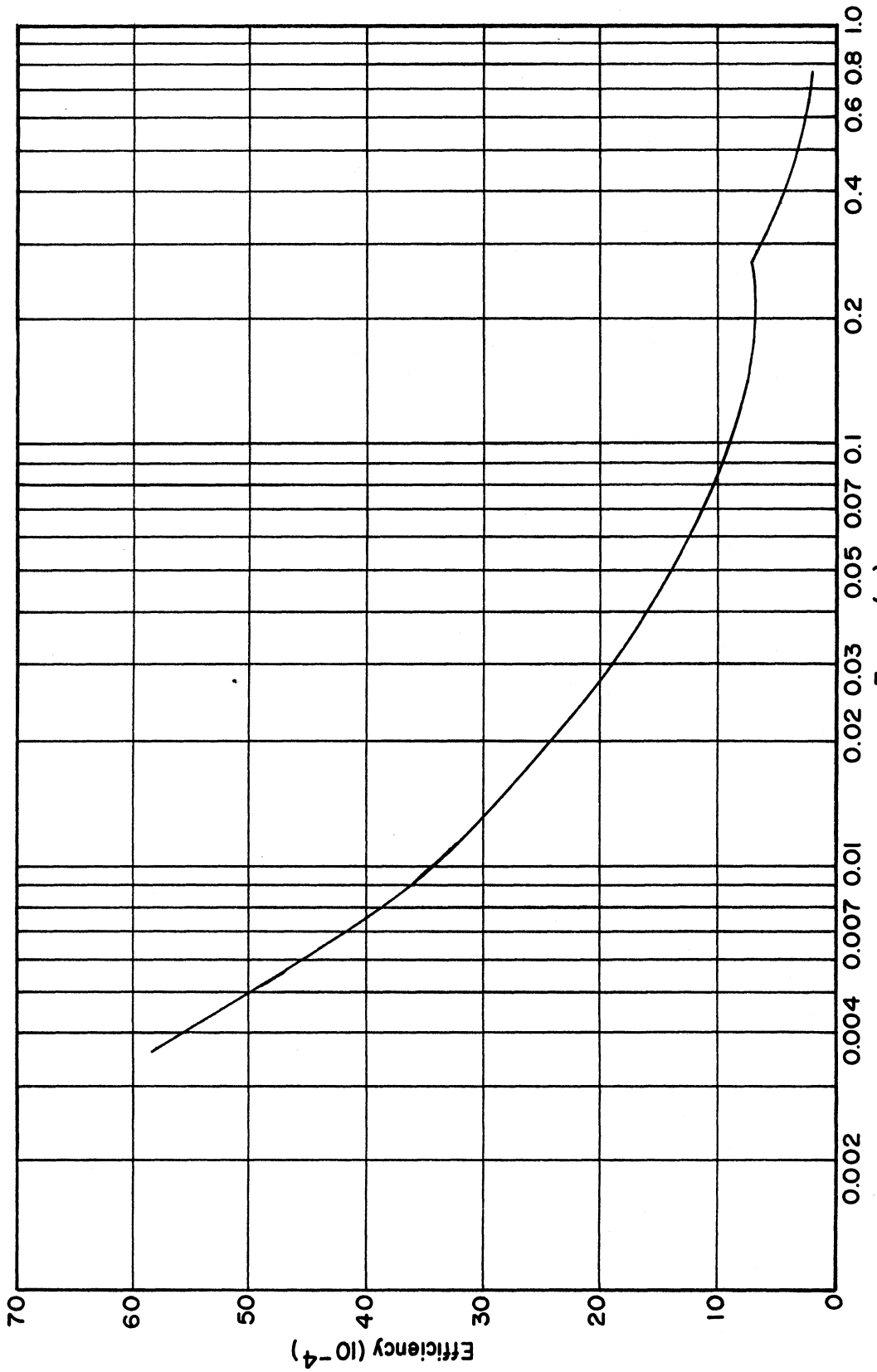

Fig. 4. Fission monitor efficiency vs. energy.

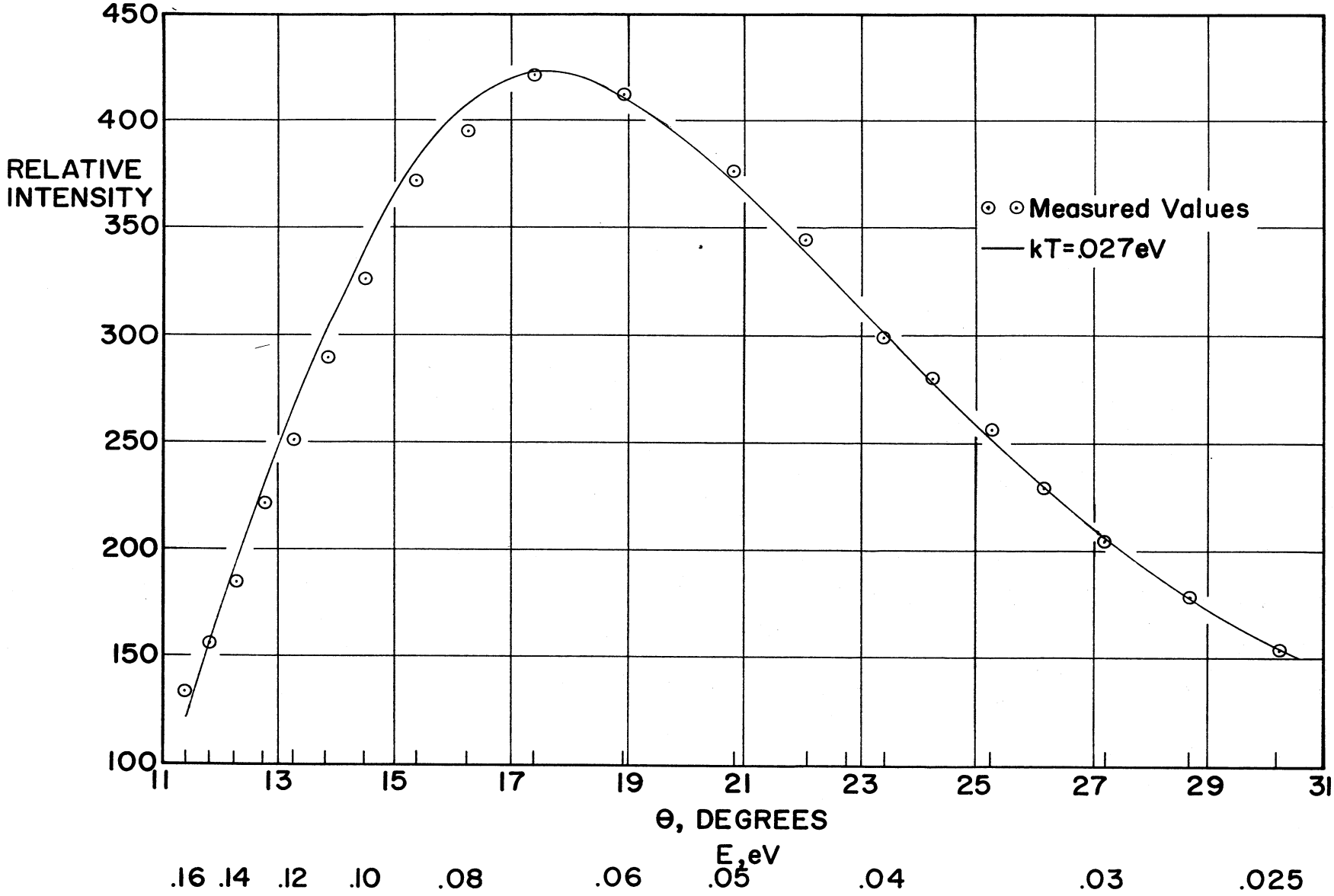

Fig. 5. Measured spectrum as a function of angle.

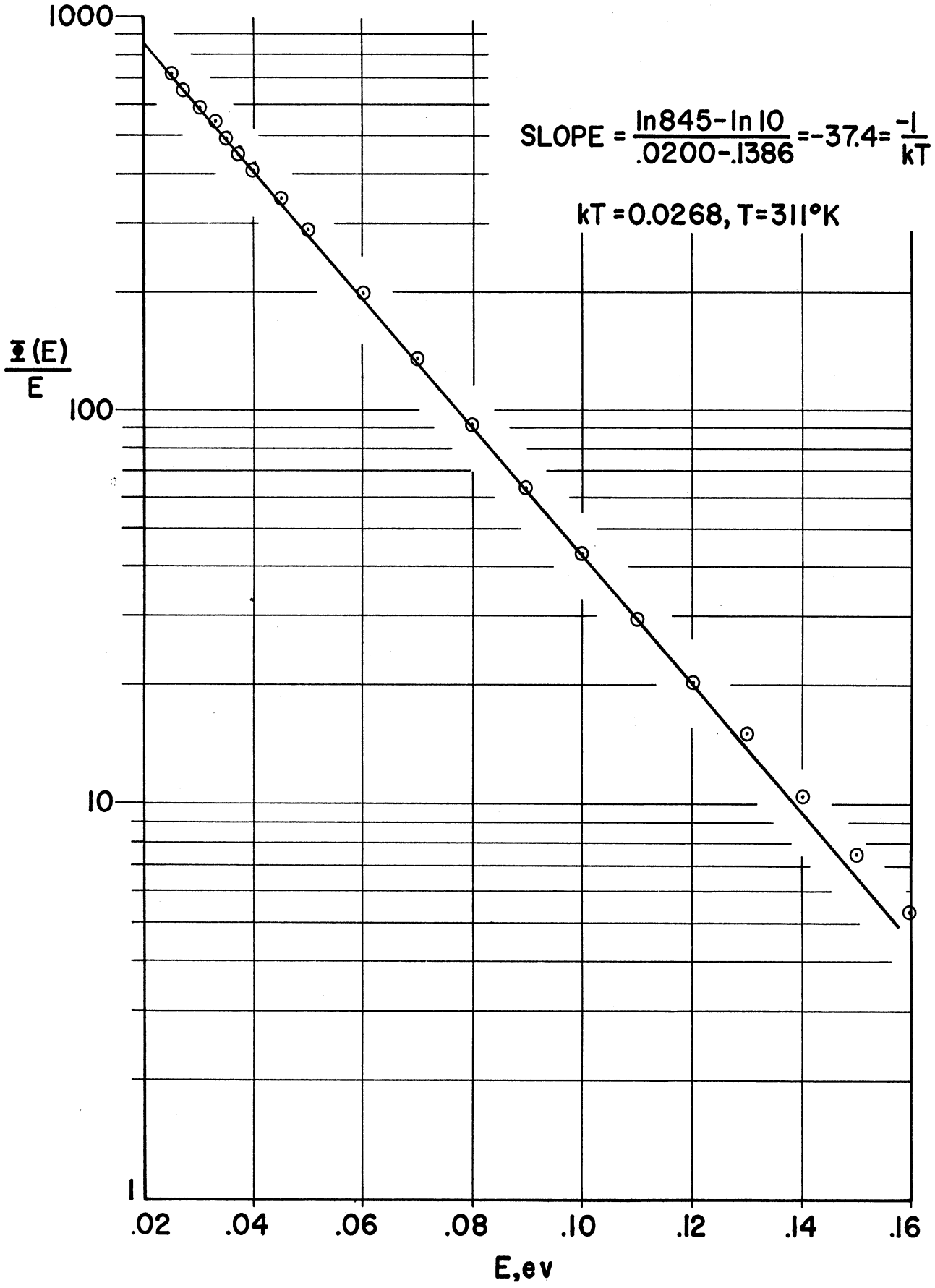

Fig. 6. Temperature determination from the energy spectrum.

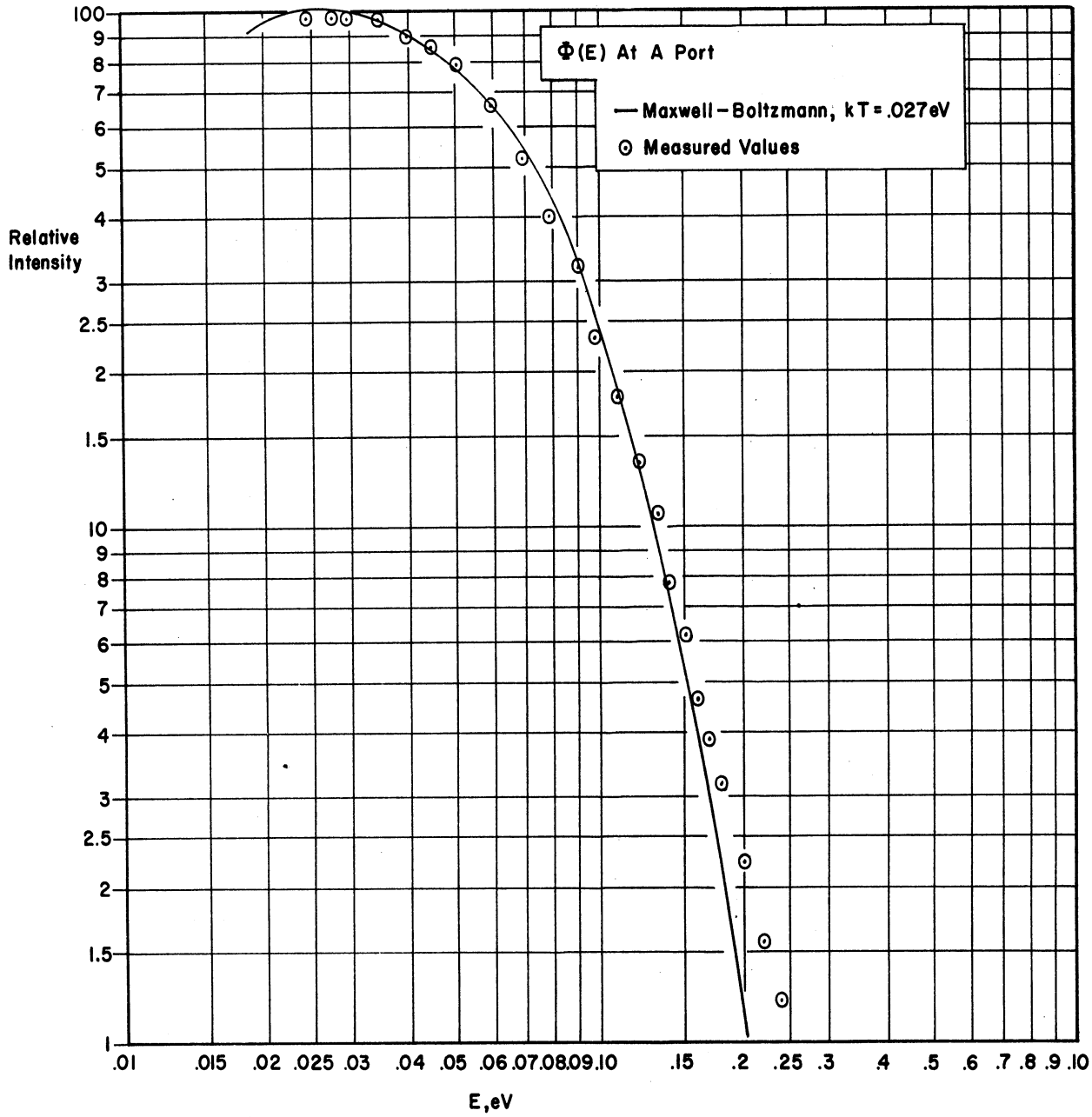

Fig. 7. Measured spectrum as a function of energy.

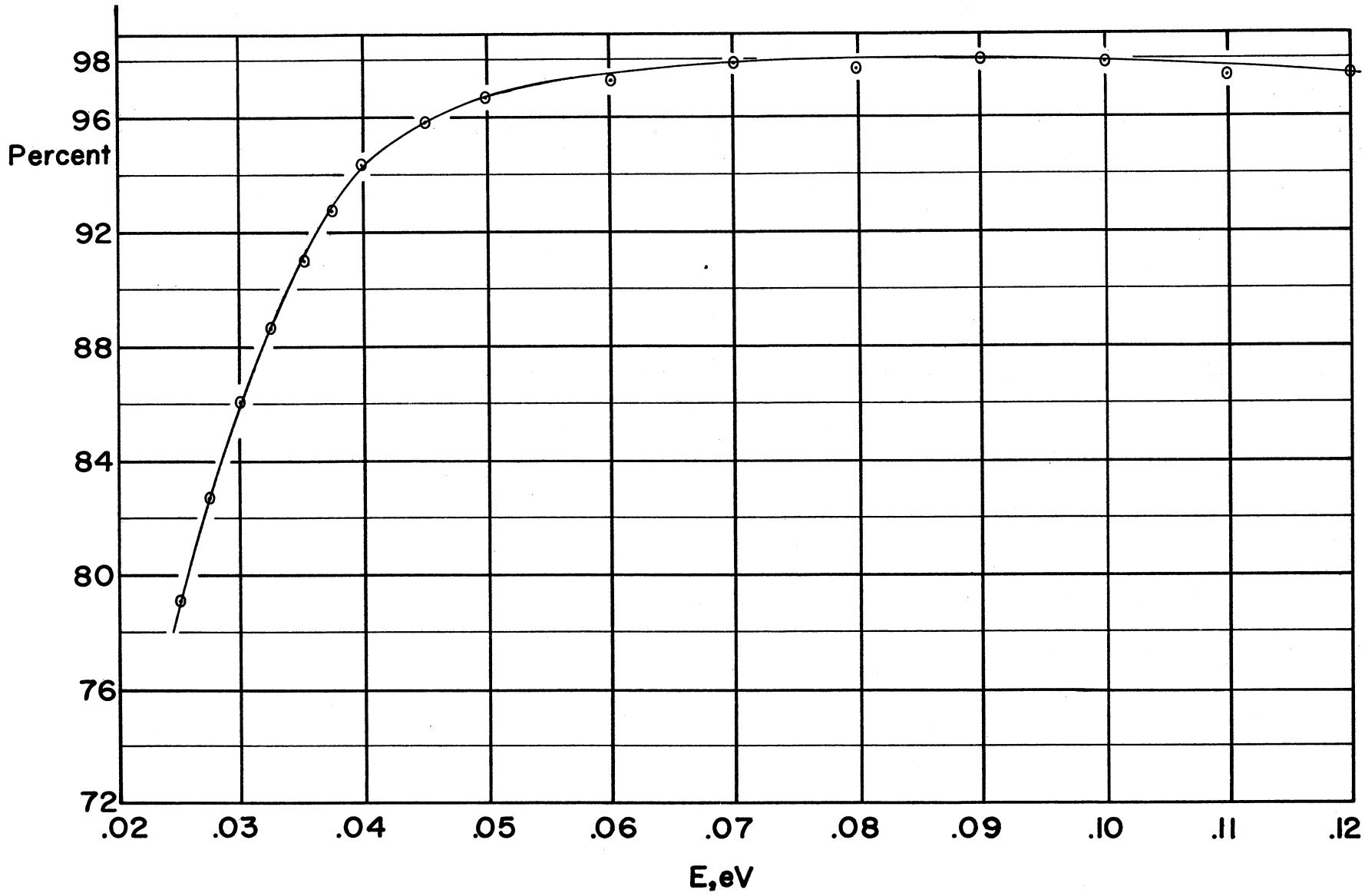

Fig. 8. Percentage of monitor count rate due to first-order neutrons.

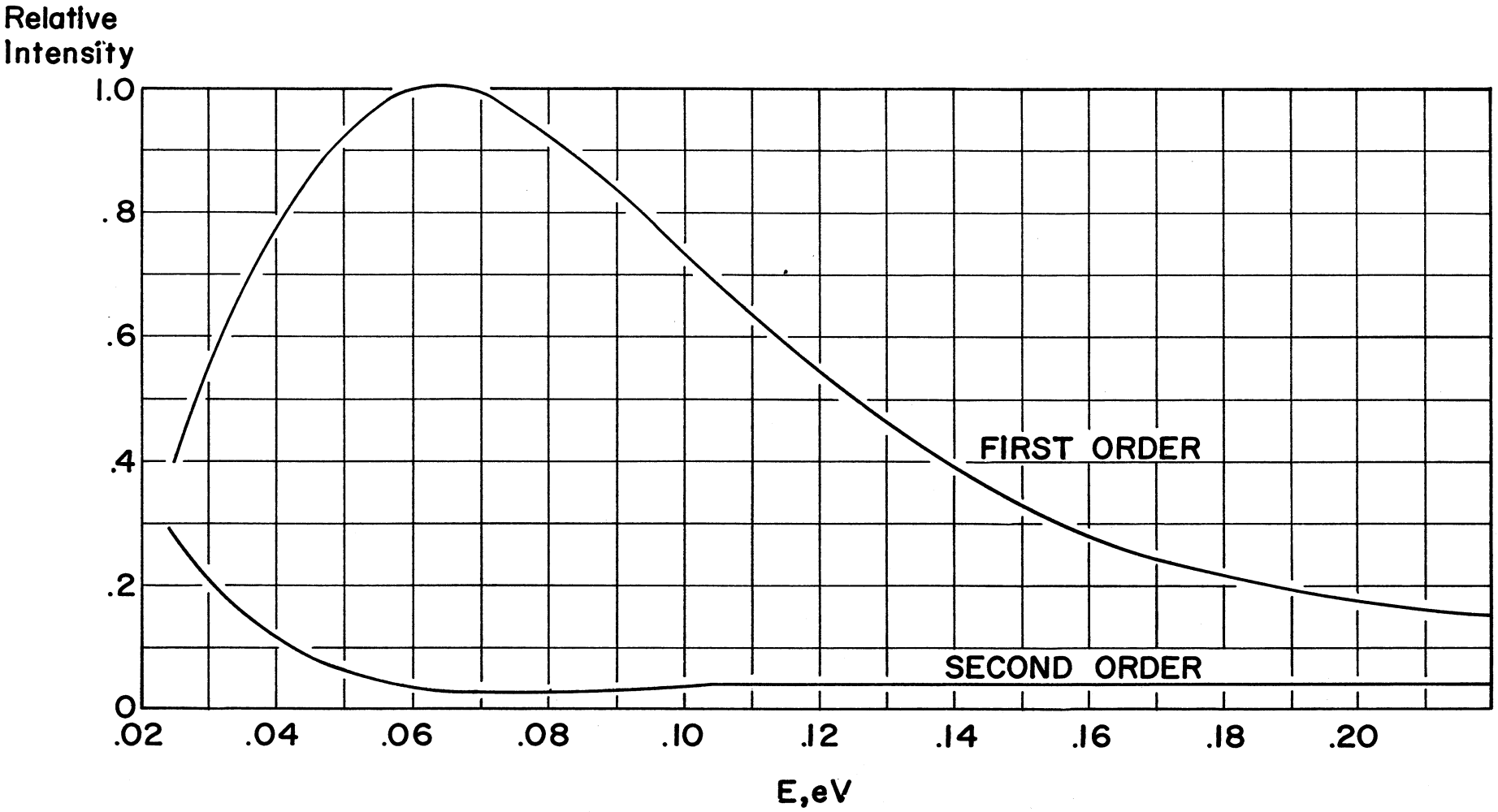

Fig. 9. Relative intensities of first- and second-order neutrons.

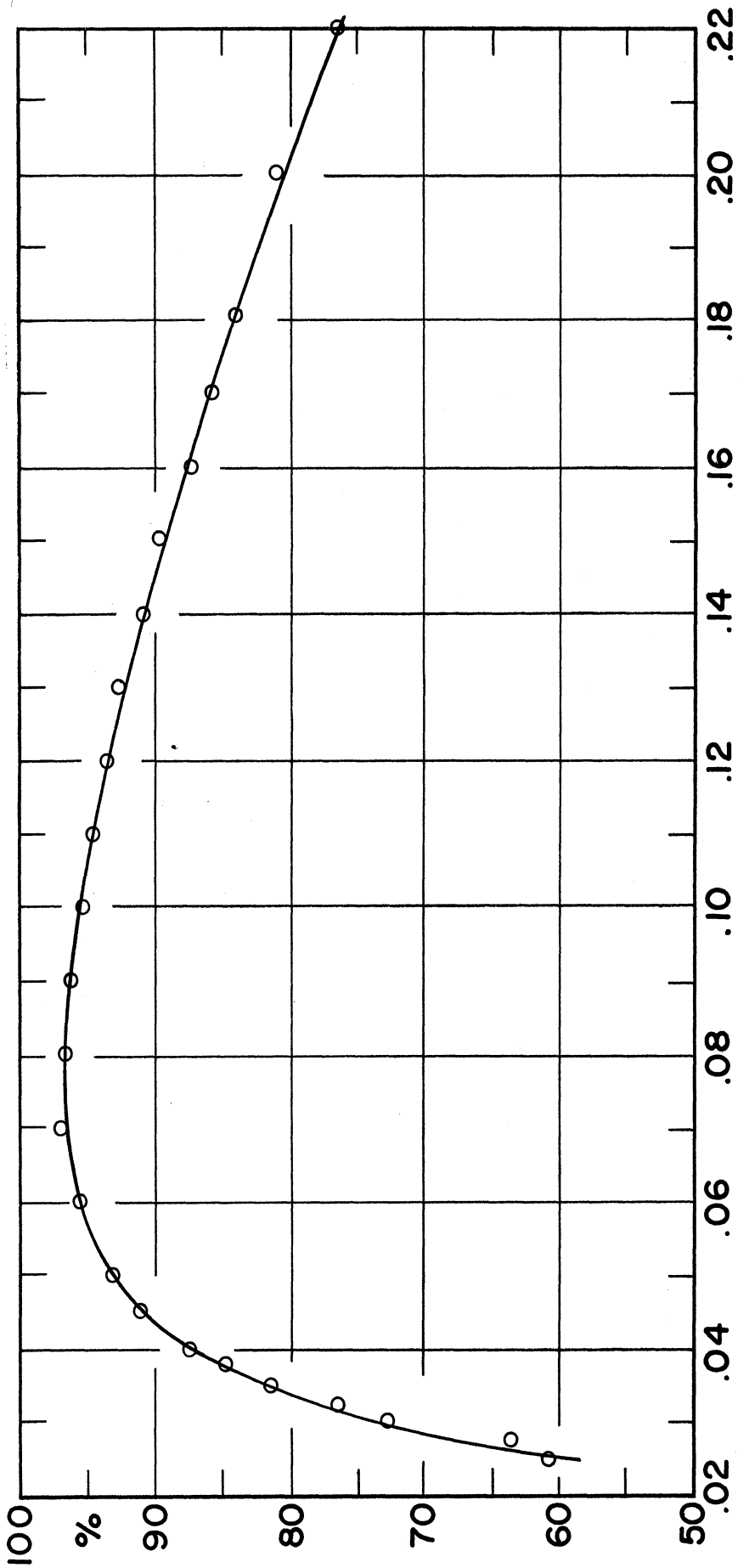

Fig. 10. Percentage of first-order neutrons in the experimental beam.